# Comparative photophysical properties of some widely used fluorescent proteins under two-photon excitation conditions

Dhruba P. Adhikari<sup>a</sup>, Gabriel Biener<sup>a</sup>, Michael R. Stoneman<sup>a</sup>, Dammar N. Badu<sup>a</sup>, Joel D. Paprocki<sup>a</sup>, Annie Eis<sup>a</sup>, Paul S.-H. Park<sup>c</sup>, Ionel Popa<sup>a</sup>, and Valerica Raicu<sup>a,b,\*</sup>

#### **ABSTRACT**

Understanding the photophysical properties of fluorescent proteins (FPs), such as emission and absorption spectra, molecular brightness, photostability, and photo-switching, is critical to the development of criteria for selection of FPs as tags for fluorescent-based biological applications. While two-photon excitation imaging techniques have steadily gained popularity – due to comparatively deeper penetration depth, reduced out-of-focus photobleaching, and wide separation between emission spectra and two-photon excitation spectra –, most studies reporting on the photophysical properties of FPs tend to remain focused on single-photon excitation. Here, we report an investigation of the photophysical properties of several commonly used fluorescent proteins using two-photon microscopy with spectral resolution in both excitation and emission. Our measurements indicate that not only the excitation (and sometimes emission) spectra of FPs may be markedly different between single-photon and two-photon excitation, but also their relative brightness and their photo-stability. A good understanding of the photophysical properties of FPs under two-photon excitation is essential for choosing the right tag(s) for a desired experiment.

Keywords: Green fluorescent protein (GFP) variants; Fluorescence; Photophysical properties; Photobleaching; Photo-switching; Brightness; Micro-spectroscopy; Two-photon (2p) excitation

<sup>&</sup>lt;sup>a</sup>Department of Physics, <sup>b</sup>Department of Biological Sciences, University of Wisconsin-Milwaukee, WI 53211, USA

<sup>&</sup>lt;sup>c</sup>Department of Ophthalmology and Visual Sciences, Case Western Reserve University, Cleveland, OH 44106, USA

<sup>\*</sup>Corresponding author's email address: vraicu@uwm.edu

## 1. INTRODUCTION

Fluorescent proteins (FPs) have proved to be powerful tools in applications where photolabeling and tracking targeted objects in living cells and organisms is desired. Following the discovery and purification of the wild-type green fluorescent protein (wtGFP) from the jellyfish *Aequorea victoria* [1], researchers have engineered a wide palette of GFP variants which possess diverse spectral characteristics, i.e., wavelength-shifted absorbance and/or emission spectra. In addition to the proteins derived from *Aequorea Victoria*, a large number of FPs which are homologous to wtGFP have been found to naturally occur in other species, e.g., Anthozoa corals [2], and Clavularia coral [3]. In recent years, researchers have expanded the FP palette by producing many variants of coral-derived FPs [2, 3].

Continued development of a vast array of spectral variants of Aequorea Victoria- or coralderived FPs [3-7] has enabled researchers to continuously develop and refine advanced fluorescence-based techniques, such as Förster (fluorescence) resonance energy transfer (FRET) for quantifying protein-protein interactions in living cells [8, 9], fluorescence correlation spectroscopy (FCS) for monitoring reaction kinetics on a molecular level in solution or within cells [10], and fluorescence intensity fluctuation (FIF) for determining the identity and stability of protein oligomers [11, 12]. Each individual protein in the vast FP library exhibits a unique combination of photophysical qualities, which include excitation and emission spectra, brightness, photostability, and sensitivity to external conditions such as pH. These differences have been exploited in several types of studies. For example, localization and colocalization studies in which different macromolecules are tracked within a cell need FPs with distinct spectra when the molecules of interest can be colocalized in the same pixel [6, 13-15]. In another example – that of FRET applied to determination of protein association stoichiometry – fluorescent proteins with different spectral properties [13, 16-20] ensure that the emission maxima of the donor and acceptor are distinguished from each other while at the same time the emission spectrum of the donor and excitation spectrum of the acceptor overlap considerably in order for resonance energy transfer (RET) to occur [8, 21]. In other experiments, it is the propensity of the fluorescent proteins to photobleach under repeated excitation with laser light that is being exploited in order to determine molecular complex stoichiometry [22, 23].

In addition to the emission and excitation spectra, a major consideration when choosing an FP for use in a fluorescence imaging technique is the overall brightness, which is a measure of the amount of light emitted by the FP. The brightness of an FP is a function of intrinsic properties of the FP, e.g., the extinction coefficient and quantum yield, and environmental factors, such as pH and temperature, and instrumentation settings, such as the excitation light intensity and excitation wavelength [24, 25]. In order to be reliably imaged, the brightness of an FP should be chosen such that it provides sufficient signal above the background noise and cellular autofluorescence signal. Choosing an FP with a relatively high brightness value allows one to lower the excitation power or expression level (or both), which is typically advantageous in many fluorescence imaging techniques.

Over the past two decades robust imaging tools have been developed using 2p excitation [8, 11, 26], and there is an abundance of studies of 2p fluorescence, such as 2p absorption cross-section of FPs [24], fluorescence dynamics of single GFP molecules [27], and single-particle photophysical properties of commercial quantum dots [28]. However, most of the time, a newly developed fluorescent protein is characterized and advertised based on its single-photon-derived spectroscopic properties, and there is still very limited information available on photobleaching

and photo-switching properties of many FPs under 2p excitation, while the 2p relative brightness of various fluorescent proteins is not consistently reported.

The relative brightness under two-photon (2p) excitation of the various FP variants, which is proportional to the 2p absorption cross-section [29], cannot be inferred directly from the relative brightness of the same FPs measured using the more common one-photon (1p) excitation. In other words, just because a particular FP is brighter than another one under 1p excitation, it is not necessarily brighter under 2p excitation. Hence, detailed measurements with 2p excitation are necessary to estimate 2p brightness, which helps researcher to choose the most appropriate FP for a 2p based fluorescence imaging technique.

While the absorption/emission spectrum and brightness are typically given the most attention when choosing the correct FP, the photostability of the FP is also an important characteristic to keep in mind when selecting the correct FP for long-term (i.e., repeated measurements) or alternating excitation wavelengths fluorescence imaging. The photostability of an FP is its ability to emit a steady fluorescence signal by resisting photophysical (or photochemical) changes during its optical excitation. Since in an excited state a molecule may be chemically reactive, fluorescent molecules are highly likely to interact with nearby molecules, such as oxygen, and thus change their properties permanently [30]. Multiple factors contribute to the overall photostability of an FP, namely the extent to which the FP undergoes photobleaching [30, 31] and photo-switching [32, 33], which will be described in more detail next.

In optical-microscopy, photobleaching is a common phenomenon that occurs when a fluorophore permanently loses its ability to fluoresce due to photo-induced chemical changes. Depending upon the molecular structure and the local environment, a fluorescent molecule can go through a certain number of excitation and emission cycles before it completely loses its ability to fluoresce. Hence, a prolonged exposure to excitation light can destroy the ability of the fluorescent molecule to fluoresce [31]. Photobleaching is a complex phenomenon that depends on multiple factors, including the power of the excitation light and the time of FP exposure to it, along with whether the surrounding environment is oxidizing or reducing. Generally, photobleaching is stronger in response to excitation wavelengths corresponding to the peak of the excitation spectrum of the FP, because the FP will go through excitation and emission cycles at a higher rate using this wavelength and hence be more prone to photobleaching.

Photo-switching occurs when fluorophores undergo a change in their spectral properties in response to irradiation with light of a specific wavelength and intensity [33-35]. Photo-switchable FPs are categorized into three broad classes: irreversibly photo-switchable from a dark to a bright state (i.e., from non-fluorescent to fluorescent), irreversibly photo-switchable from one emission color to another, and reversibly photo-switchable enabling bright-to-dark switching capability [34, 36]. In the case of irreversibly photo-switchable from a dark to a bright state, the peak wavelength of the excitation spectrum changes and, sometimes, can shift to a different excitation wavelength as the chromophore changes from the neutral (protonated) state to anionic (deprotonated) state in response to the irradiation of light of certain wavelength and intensity [36, 37].

Both attributes described above (i.e., photobleaching and photo-switching), are the two main factors that determine the photo-stability of an FP. Lack of photo-stability in an FP is often detrimental but sometimes desirable in measurements. For a gamut of fluorescence-based techniques, such as FRET [21, 38, 39], FCS [10, 40], and fluorescence intensity fluctuation (FIF) spectroscopy [11, 12], FPs with high photostability are preferable. Multiple scans or long-term scans of a fixed region of interest is common in these methods to follow the dynamic nature of the

biological system of interest at the molecular level. In these techniques, it is expected that the first excitation does not significantly alter the usual behavior of the FP in the next excitation.

There are also situations when photobleaching is useful. For example, fluorescence recovery after photobleaching (FRAP) [41], which allows one to monitor the diffusion of fluorescent molecules as they diffuse into a photobleached region immediately following excitation due to high-intensity laser light. In addition, identification of the number of molecules within a supra-molecular complex has become possible by counting photobleaching steps in single-molecular complex measurements [22, 23]. Likewise, development of photo-switchable FPs has helped advance fluorescence imaging techniques and permitted optical control of protein activity [32, 42], information storage [43], and super-resolution imaging [33]. Having a good understanding of the photophysical properties of FPs, therefore, is essential for choosing the right tag(s) for a desired experiment. Numerous studies have been published characterizing the photophysical properties of GFP variants using confocal microscopy [44, 45].

In this study, we present a comparative analysis of the photophysical properties under twophoton excitation of some widely used FPs. These investigations have been performed via twophoton micro-spectroscopy with spectral resolution in both the excitation and emission channels [8, 46], with the aim of providing guidelines for screening of FPs as tags in various 2p fluorescence microscopy applications. We used purified FPs embedded in a polyacrylamide gel, which allowed us to scan the same molecules successively a number of times in order to measure the fluorescence intensity as a function of scan number, as well as excitation and emission wavelengths. By quantifying the fluorescence intensity and monitoring changes in the emission and excitation spectra of an FP occurring due to repeated scans using a pair of excitation wavelengths, we were able to quantify the level of photobleaching for each FP as well as to determine whether a particular FP underwent photo-switching. We have also estimated the 2p brightness (relative to mEGFP) of each FP by performing z-stack acquisitions of FP-doped gels (see section 2.5 below) using an excitation wavelength that corresponds to the peak of the FP's 2p excitation spectrum. Comparing our 2p-excitation measurements to single-photon measurements reported in the literature, we conclude that not only the excitation (and sometimes emission) spectra, but also the photobleaching, photo-switching, and brightness properties of FPs may be markedly different under single-photon and two-photon excitation.

## 2. MATERIALS AND METHODS

## 2.1. Preparation of stock solutions

For the experiments presented herein, we prepared several stock solutions for use in making the polyacrylamide gels embedding fluorescent proteins. All reagents were either purchased from Fisher Scientific, or otherwise specified below. A 10% ammonium persulfate (AP; Sigma-Aldrich, MO) solution, prepared by dissolving 0.1 g of AP in doubly distilled (DD) water to a final volume of 1 ml, was used for inducing the polymerization of the polyacrylamide (PAA) solution. A 30% PAA stock solution was prepared by dissolving 6 g of powder polyacrylamide (PAA; Sigma-Aldrich, MO) and 0.3 g of bis-acrylamide (BAA; Sigma-Aldrich, MO) in DD water to a final volume of 20 ml of solution. This solution was then mixed thoroughly using a 3D nutating shaker (BioMixer; Benchmark Scientific Inc., NJ) for at least one hour, and thereafter the solution was degassed under a vacuum of 0.1 m³/s for 30 minutes at room temperature. Finally, a number of different phosphate-buffered saline solutions were prepared at various pH values; the final pH of

each solution was achieved by addition of NaOH or HCl to a stock solution of Dulbecco's phosphate buffered saline (DPBS; REF: 14190-144, Life Technologies, NY). All stock solutions were stored at 4°C and were used in the preparation of FP-doped polyacrylamide gel samples (see section 2.3 below) for up to two weeks after their initial preparation date.

## 2.2. Surface cleaning

All glass slides and coverslips were cleaned following a rigorous, multi-step process before use. A clean surface is essential to prevent undesirable signals that may arise due to excitation of unwanted surface impurities. For example, organic or inorganic matter located at the plane of excitation (i.e., on the surface), during the fluorescence measurements. In addition, preparation of slides and coverslips in this manner also helped to prevent binding of the FPs to the surface. For this, glass slides were kept in acetone for at least 24 hours. The coverslips were kept in piranha solution (a 3:1 mixture of sulfuric acid and 30% hydrogen peroxide) for 24 hours, and then rinsed with DD water, and acetone sequentially. Next, both glass slides and coverslips were dried with clean, dry, compressed air and then treated with oxygen plasma by exposing them to the wire electrode of a plasma generating device (BD-20AC Laboratory Corona Treater; Electro-Technic Products, IL) for approximately 15 min [47, 48]. The cleaned slides were used immediately, i.e., FP-doped polyacrylamide gel (see section 2.3 below) samples were deposited on the slides within minutes after being treated with the oxygen plasma.

# 2.3. Preparation of FP-doped polyacrylamide gel samples

The fluorescent proteins mGFP2 [6, 8], mEGFP [49-51], mYFP [5], mCitrine [52, 53], SYFP2 [54], mVenus [52, 54], mTurquoise (mTq) [55], mCerulean3 [7], and mTFP1 [3] were expressed and purified using standard bacterial expression systems. Note that the "m" before the fluorophore name refers to the fact that it contains the A206K point mutation, to reduce dimerization [56]; the same mutation was incorporated also into SYFP2, although in the literature "m" is usually omitted from its name. The plasmid DNA was transformed into C41(DE3) chemically competent cells, which were then grown in LB buffer at 37 °C, in the presence of antibiotic (carbenicillin), until the culture showed an absorption optical density at 600 nm O.D. <sup>600</sup> = 0.6. Following the growth phase, protein overexpression was induced by treating the cultured bacteria with 1mM IPTG (VWR Life Science) overnight at 25 °C. Finally, chloramphenicol was added at a final concentration of 200 µg/ml for 2 hours, to allow for fluorophore maturation. Cells were then lysed chemically (with DNAse, RNAse, and lysozyme) and mechanically (through sonication). The soluble fraction was passed through a Ni-NTA column (Fisher Scientific), which bound the protein of interest through their polyhistidine tag. Following washing and elution with 250 mM imidazole, the protein of interest was further purified using size exclusion chromatography (AKTApure, GE with S300 column). Unless otherwise mentioned, all chemicals and competent cells were purchased from Sigma-Aldrich.

Purified proteins were then embedded separately at desired concentrations in polyacrylamide (PAA) gel following a method by Dickson et al [57] and using the stock solutions described in section 2.1. The average size of the gel pores may be tuned from 2 nm to several hundred nm in diameter [57, 58] by altering the acrylamide and cross-linker final concentrations. In all of our samples, we used final concentrations of 15% (w/w) for the acrylamide gel and 5% (w/w) cross-linker to achieve pore sizes of approximately 2 nm.

The FP-doped PAA gel was prepared by first adding 244  $\mu$ L DPBS buffer of known pH, 244  $\mu$ L of 30%-PAA stock solution, 12.5  $\mu$ L of 40  $\mu$ M FP of interest, 2.4  $\mu$ L of 10% AP stock solution, and 0.5  $\mu$ L Tetramethylethylenediamine (TEMED; Sigma-Aldrich, MO) sequentially to an Eppendorf tube to achieve a solution with a final FP concentration of 1  $\mu$ M. Thereafter, the solution was vortexed for 5 to 10 seconds to ensure homogeneity. The gel was left undisturbed at room temperature for three minutes after vortexing, and then 7.5  $\mu$ L of the gel was pipetted onto the surface of a freshly cleaned glass slide before it being sandwiched between the glass slide and a clean coverslip (see Section 2.2 above). Approximately three minutes after the sample was placed between the glass slide and coverslip, the sample was fully polymerized. In order not to avoid photobleaching of the FPs before micro-spectroscopic measurements, we covered the slide with aluminum foil.

Each FP sample was prepared and measured under the same environmental conditions. Exposure to fluorescent light with wavelengths which could potentially photobleach the FPs was avoided by preparing all samples in a room where the only illumination was from a dim yellow fluorescent light bulb. The fluorescent-protein-doped samples were measured immediately after preparation to avoid complete evaporation of water from the gel. The measurements, which took 3 to 4 hours, were performed in a dark room. Finally, positioning the FP-doped gel within the focal plane of the optical micro-spectroscope (see Section 2.4 below) was accomplished using a lower laser intensity (compared to the actual measurements) to avoid unwanted photophysical effects before the actual measurements were performed.

# 2.4. Two-photon (2p) excitation micro-spectroscopy measurements of FP-doped PAA gel

The instrumentation used to carry out 2p excitation micro-spectroscopic measurements in this investigation has been described previously [59]. Briefly, measurements were performed with a 2p optical micro-spectroscope comprised of an inverted Nikon Eclipse Ti<sup>TM</sup> microscope (Nikon Instruments, Inc., Melville, NY) and an OptiMiS<sup>TM</sup> scanning/detection head (Aurora Spectral Technologies, Grafton, WI) equipped with a line-scan module. A mode-locked Ti-Sapphire laser (Mai Tai<sup>TM</sup>, Spectra Physics, Santa Clara, CA) which generates 100 fs pulses with central wavelengths tunable between 690 nm and 1040 nm was used for the fluorescence excitation. The excitation beam was focused into a line in the sample by an infinity corrected oil-immersion objective with 100× magnification. The OptiMiS detection head used a non-descanned detection scheme in which emitted light was spectrally resolved by passing it through a transmission grating and projecting onto a cooled electron-multiplying charge-coupled device (EMCCD) iXon Ultra 897 camera (Andor Technologies, South Windsor, CT). The emission wavelengths of the fluorescence were separated as a function of pixel position on the EMCCD array. For all the measurements we have used a fixed spectral resolution of 5 nm, which allowed us to capture 2D fluorescence images for 40 different wavelength channels ranging from 415 nm to 615 nm.

To characterize the photostability of the fluorescent molecules, we performed a series of micro-spectroscopic measurements (what is hereby referred to as an excitation time series) using two different excitation wavelengths; each series of measurements was performed on the same region of interest (ROI) within a particular sample. Specifically, an excitation time series was carried out on a sample by first scanning the sample ten successive times using a fixed wavelength (e.g., 960 nm for mGFP2). Then, an additional set of ten scans was performed while using a different excitation wavelength (e.g., 800 nm for mGFP2). This process of alternating between a series of ten scans at two different excitation wavelengths was repeated two (or three) additional

times, meaning that each sample was scanned in the same location a total of thirty (or, in some cases, forty) times for each of the two different excitation wavelengths, to detect possible effects of photo-switching. For both excitation wavelengths, an average laser light power (measured in the sample plane) of 200 mW/line (corresponding to 0.5 mW per pixel) and integration time of 200 ms/line were used. The excitation wavelengths for a particular FP were chosen to be similar (or equal) to those previously used in FRET [8, 39, 60, 61] or other fluorescence-based studies [11, 62, 63], and which, in certain cases, have caused the FP to elicit some peculiar behavior, e.g. photo-switching. Immediately before and after each series of micro-spectroscopic measurements were performed, an excitation spectrum of the sample was acquired, in order to study the effect of successive excitations on the spectral characteristics of the FPs. The excitation spectra were acquired by scanning the sample multiple times, each time with a different wavelength, ranging from 780 nm to 1000 nm in increments of 20 nm. The average laser power and integration time were kept constant for each excitation throughout the course of an excitation spectrum acquisition, namely at 100 mW/line and 50 ms/line, respectively. From the 2p excitation time series, the extent of photobleaching for each FP was quantified by calculating the fraction of total fluorescence lost during first 10 the first excitation scans, as follows:

$$R_{2p}^{PB} = \frac{TF_1 - TF_{10}}{TF_1} \times 100 \tag{1}$$

where  $TF_1$  and  $TF_{10}$  represent the total fluorescence (integrated over the entire emission spectrum) detected after the  $1^{st}$  and  $10^{th}$  scans, respectively, of the sample using an excitation wavelength ( $\lambda_{exc,max}$ ) corresponding to the peak wavelength of the excitation spectrum of the particular FP under study.

To test for the expected quadratic dependence of the fluorescence emission vs. laser pulse energy for two-photon excitation, we used mEGFP prepared as described in Section 2.1. The sample was excited at 960 nm at several average excitation powers ranging from 50 mW per entire laser line to 400 mW/line in increments of 50 mW/line. To minimize the unwanted photobleaching we avoided taking multiple measurements from the same spot of the fluorescent sample. The resulting log-log plot (see Supplementary Fig. 1) of total fluorescence emission as a function of the laser pulse energy exhibited a quadratic dependence, as expected.

# 2.5. Measurements of FP-doped PAA gel for 2p relative brightness determination

To determine the 2p brightness (relative to mEGFP brightness) of all the FPs investigated, microspectroscopic measurements were performed on FP doped gel using a similar imaging system as described in Section 2.4 above, except that the OptiMiS<sup>TM</sup> scanning/detection head was modified to employ a pseudo-line-scan protocol. In this protocol, the appearance of a line was generated by rapidly sweeping a point-focused laser beam along a line in the sample, while integrating the signal on the camera during the course of the sweep. The inverted microscope used in conjunction with the OptiMiS<sup>TM</sup> scanning/detection head in this system was a Zeiss Axio Observer equipped with a water-immersion objective with 63× magnification and NA= 1.2.

In order to assure the FPs were uniformly distributed throughout the gel, z-stack acquisitions were performed, in which micro-spectroscopic measurements were taken at multiple planes within the FP-doped gel. Specifically, the initial measurement was taken at a plane within the gel located  $\sim$ 5  $\mu$ m away from the coverslip-gel interface. Then, the microscope objective was moved by 2  $\mu$ m in the z-direction such that the focus of the laser was moved further into the gel, and micro-spectroscopic measurements were taken again. This process was repeated until the focus

of the laser beam reached to  $\sim$ 5 µm away from the top gel-microscope slide interface. For all z-stack acquisitions, an average laser power of 12 mW/point and a dwell time of 195 µs/point were used. The excitation wavelengths were chosen to correspond to the peak of the FP's excitation spectra (e.g., an excitation wavelength of 960 nm was used for mEGFP and 800 nm for mGFP2).

## 2.6. Spectral unmixing and calculation of total emission intensity

Emission spectra of the FP-doped polyacrylamide (PAA) gel obtained using the microspectroscopic measurements described above contained contributions not only from the FPs embedded in the gel but other sources as well. For example, the polyacrylamide gel was also seen to be excited in the optical micro-spectroscope. In order to separate the FP signal from the other contributing sources of signal, a previously described spectral unmixing procedure was applied to the composite emission spectra [13] obtained from each gel sample. Briefly, a single composite emission spectrum was obtained from a micro-spectroscopic scan by averaging the intensity values over a 1000 pixels region for each wavelength channel obtained from the scan. Then the composite emission spectrum was deconvoluted into the FP and PAA components using a least-squares fitting algorithm [13, 46, 64] (implemented using Solver in Microsoft Excel<sup>TM</sup>) along with separately determined elementary spectra of the FP and PAA gel. In order to determine the elementary spectra of the FP and the PAA gel, separate micro-spectroscopic measurements were performed on PAA gel alone (i.e., without FP embedded in it) and the FP in solution (i.e., not embedded in gel); each of the elementary spectra was normalized to their respective maximum intensities before being used in the unmixing algorithm.

The unmixing procedure provided two best-fit parameters, k<sup>FP</sup> and k<sup>gel</sup>, which are proportional to the emission intensity of the FP and PAA gel, respectively. In other words, k<sup>FP</sup> and k<sup>gel</sup> are the parameters multiplying each respective elementary spectrum comprising the theoretical function used to fit the measured composite emission spectrum. Once it was extracted using the unmixing procedure, the k<sup>FP</sup> value was multiplied with the spectral integral of the FP (i.e., area underneath the elementary spectrum of the FP) to obtain the total emission intensity (also known as total fluorescence) of a given FP. Under certain experimental conditions – for example, in measurements using relatively low excitation powers or short exposure times (or both) –, there was no detectable contribution of the PAA gel to the emission spectra of the FP-doped PAA gel. In those situations, the FP signals were separated from the measured emission signal simply by subtracting the minimum intensity of the emission spectrum from the observed emission signals, which corresponds to the DC-bias and shot noise distribution of the camera. Then the total detected emission intensity was calculated by integrating the entire FP spectrum (after background subtraction).

#### 3. RESULTS AND DISCUSSION

In order to quantify and compare the photophysical properties, i.e., the excitation and emission spectra, molecular brightness, level of photobleaching and photo-switching, and sensitivity to pH, of widely used FPs, we performed a series of two-photon (2p) micro-spectroscopic scans of FPs samples according to the procedure described in detail in Section 2.4 (and which we refer to as an excitation time series). The FPs samples were PAA gel doped with one of the following FPs: mGFP2 [6, 8], mEGFP [49-51], mYFP [5, 65], mCitrine [53], SYFP2 [54], mVenus [54], mTurquoise (mTq) [55], mCerulean3 [7], and mTFP1 [3]. These FPs were separately immobilized

in PAA gel, as described in Section 2.3, to reduce their molecular diffusion [57] before and during the series of measurements.

The degree of 2p photobleaching of each FP was quantified using the *relative two-photon* photobleaching ( $R_{2p}^{PB}$ , see Eq. 1 above), which we defined as the fraction of total emission intensity lost after the first ten successive excitations using an excitation wavelength corresponding to the excitation maximum of each FP. The relative 2p photobleaching reported for a particular FP was determined by averaging the  $R_{2p}^{PB}$  over multiple sets of excitation scans performed on different samples containing the tested FP. It should be noted that for samples that exhibited strong photoswitching properties, we were not able to calculate a value for  $R_{2p}^{PB}$ , as the reduction of the total intensity during the repeated time series excitations was the result of the combined effect of photobleaching and photo-switching.

All the properties investigated are first presented and discussed in detail in the following sub-sections and then summarized in Table 1 appended at the end of the Results section.

## 3.1. Photostability of FPs investigated using two-photon excitation time series

## 3.1.1. Green variants of wtGFP

Fig. 1 illustrates the results obtained from mGFP2-doped PAA gel samples subjected to an excitation time series consisting of ten successive excitation scans at 960 nm alternating (four times) with ten successive excitation scans at 800 nm. As seen in panel a, the total emission intensity decreased during the course of the ten successive excitation scans. The rate of decrease in the total emission intensity was higher for excitation at 800 nm in comparison to excitation at 960 nm. In addition, (i) the fluorescence intensities acquired upon excitation at 960 nm jumped significantly upwards when those measurements followed the excitation scans at 800 nm, (ii) while excitation at 960 nm had little to no effect on the results of subsequent 800 nm excitation series. This second observation suggests that, while the slight decrease in emission intensity within each set of ten 960 nm excitation scans was caused primarily by photobleaching, the marked decreasing trend in the intensities during each of the ten excitation scans at 800 nm was caused instead by photo-switching induced by excitation at 800 nm.

The above interpretation is also supported by the results shown in panels b, c and d of Figure 1, as follows. As seen by comparing the two mGFP2 excitation spectra of Fig. 1b (one obtained before and one after performing the excitation time series on the sample), a shift in the maximum two-photon excitation wavelength from 800 nm to 960 nm (or perhaps an even longer wavelength) occurred as a result of repeated excitation scans. Fig. 1c-d shows comparatively the changes in fluorescence intensities at excitation wavelengths of 960 nm (panel c) and 800 nm (panel d) at the beginning and the end of the entire excitation time series. Notice the unchanged maximum emission wavelength, which may imply that the new mGFP2 species resulting from photo-switching may in fact be different forms of the same fluorescent protein, as described below.

The cause for the photo-switching observed in the mGFP2 sample can be ascertained from previously made observations regarding wtGFP [66-68], as follows. The wtGFP chromophore exists in either a neutral (i.e., protonated) form, which has a single-photon (1p) excitation maximum at 397 nm, or an anionic form that is maximally excited at 475 nm. Upon either single photon excitation (at 397 nm) or two-photon excitation (at about 800 nm), the neutral chromophores can undergo photoisomerization and be converted to their anionic form. The equilibrium between the neutral and anionic states is regulated by a complex hydrogen-bond

network which forms between the amino acids of the fluorophore and surrounding water molecules. The breaking and forming of multiple hydrogen bonds facilitates a proton transfer from the side chains of the fluorophore to the chromophore, resulting in the stabilization of the chromophore in the anionic state [67]. By replacing the serine amino acid at position 65 in the wtGFP sequence with threonine [4] (i.e., the S65T mutation, possessed by, e.g., the EGFP variant), the population of neutral (protonated) chromophores, and thereby the excitation peak at 397 nm, is effectively suppressed; this peak suppression occurs due to a rearrangement of hydrogen bond patterns in the nearby amino acid Glu222, which in turn suppresses the negative charge on Glu222 and allows the chromophore to assume an anionic form. We confirmed the decrease of the neutral population of chromophores due to the S65T mutation by observing the effect of applying the excitation time series to EGFP-doped PAA gel (see Supplementary Fig. 2). It is apparent from the results shown in Supplementary Fig. 2 that no photo-switching is observed during excitation time series measurements of EGFP-doped PAA gel, due to the fact that all chromophores are presumably already in the anionic form prior to being exposed to any 800 nm excitation scan. However, mGFP2, which does not have the S65T mutation and therefore maintains a population of chromophores in the neutral form (and maintains an excitation peak at 397 nm in 1p excitation and 800 nm in 2p excitation), is susceptible to ionization when excited using 2p excitation at 800 nm. This ionization causes the significant amount of photo-switching seen in Fig. 1a and 2a and the shift in excitation spectrum seen in Fig. 1b.

These results suggest that mGFP2 could be used in experiments where photo-switching is useful or necessary. Nevertheless, it needs to be used with caution in other studies where such effects might introduce challenges, such as in FRET experiments that rely on two different excitation wavelengths to determine both FRET efficiency and concentrations of donors and acceptors [8, 19, 61, 69]. To further explore the latter case, we performed experiments (illustrated in Fig. 2) in which the order of the wavelengths used in the excitation time series was switched. While a reduction in intensity is still seen during the repeated excitation scans, exciting first at 800 nm appears to have photo-switched some of the fluorescent proteins to the subspecies (i.e., from protonated state to deprotonated state) the one that is excited more efficiently at 960 nm prior to the first excitation scan at 960 nm being measured. Therefore, scanning the sample using this order of excitation wavelengths (i.e., 800 nm first, and 960 nm second) may lead to a false impression that mGFP2 emits more upon excitation at 960 nm than compared to excitation at 800 nm. However, if we compare Fig. 2c and Fig. 1c, we conclude that the emission intensity at an excitation of 960 nm was actually less than that observed after the successive excitations at 800 nm. Hence, in general, for long-term measurements with multiple-wavelengths excitations, it is always better to start the measurement with the excitation wavelength that produces minimal unwanted photophysical effects (in this case, to avoid significant effects in the subsequent measurements).

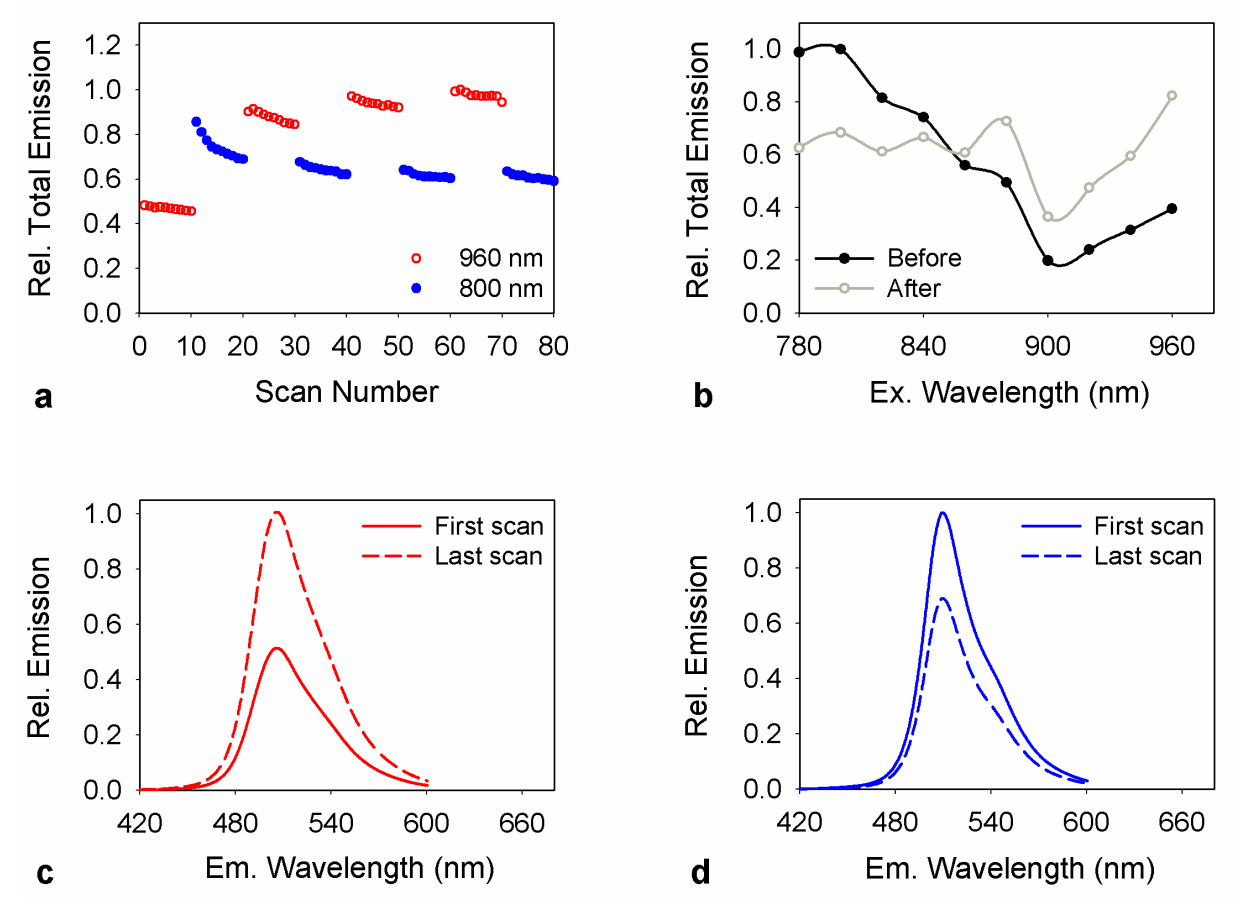


Figure 1. Response to repeated two-photon excitation scans of PAA gel doped with monomeric Green Fluorescent Protein 2 (mGFP2) at pH 8. (a) Changes in total emission intensity (integrated over all emission wavelengths) induced by acquiring time series of ten successive excitation scans at 960 nm (empty red circles), followed by ten successive excitation scans at 800 nm (filled blue circles). The couple of 960nm/800-nm scans was repeated three additional times, for a total of forty excitation scans at each wavelength. The total emission was computed by integrating over the entire emission spectrum. (b) Comparison of two-photon excitation spectra, measured as emission intensity, before (black line with filled circles) and after (gray line with empty circles) the sample was subjected to the entire excitation time series as shown in (a). (c) Emission spectra of mGFP2 observed at an excitation wavelength of 960 nm, where the red solid line represents the first and the red dashed line represents the last emission spectrum obtained from the repeated excitation time series. (d) Emission spectra of mGFP2 observed upon excitation at 800 nm, where the blue solid line represents the first and the blue dashed line represents the last emission spectrum obtained from the repeated time series excitations. All plots were normalized to the maximum value observed in the respective data set. The final concentration of mGFP2 in the FP-doped polyacrylamide gel was 1 µM. For repeated excitation time series, the integration time of the camera was 200 ms and the excitation power per entire excitation line was 200 mW (corresponding to 0.5 mW per pixel). For the excitation spectra measurements, the integration time was 50 ms, and the excitation power was 100 mW/line.

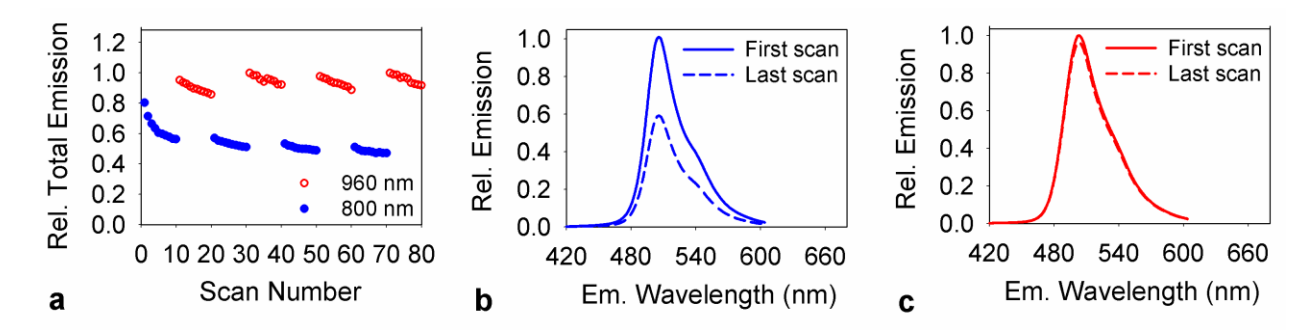


Figure 2. Changes in photophysical behavior of mGFP2 caused by switching the order between the two excitation wavelengths. (a) Changes in total emission intensity (integrated over the entire emission spectrum) induced by acquiring time series of ten successive excitation scans at 800 nm (filled blue circles), followed by ten successive excitations scans at 960 nm (empty red circles). The couple of 800-nm/960-nm scans was repeated three additional times, for a total of forty excitation scans at each wavelength. The total emission was computed by integrating over the entire emission spectrum. (b) Emission spectra of mGFP2 observed upon excitation at 800 nm, where the blue solid line was the first and the blue dashed line was the last emission spectrum obtained from the repeated time series excitations. (c) Emission spectra of mGFP2 observed at an excitation wavelength of 960 nm, where the red solid line represents the first and the red dashed line represents the last emission spectrum obtained from the repeated excitation time series. All resulting plots were normalized relatively to the maximum fluorescence observed in the respective data set. The final concentration of mGFP2 in the FP-doped polyacrylamide gel was 1 μM and pH value of the sample was 8. For repeated excitation time series, the integration time of the camera was 200 ms and the excitation power per entire excitation line was 200 mW (corresponding to 0.5 mW per pixel).

## 3.1.2. Cyan fluorescent proteins

Unsurprisingly, not all GFP variants exhibited the same photophysical behavior. For example, a cyan variant of wtGFP known as monomeric Turquoise (mTq) (see Fig. 3), when exposed to alternating time series of excitation scans using a pair of wavelengths (920 nm and 880 nm) that correspond to the peaks in its two-photon excitation spectrum (Fig. 3b), underwent marked photobleaching, but no noticeable photo-switching, i.e., there was no increase in fluorescence signal under 920 nm excitation that followed 880 nm excitation scans (Fig. 3a), and no shift of excitation maxima (Fig. 3b). Similar results were obtained when switching the order of the excitation wavelengths in the excitation time series (Supplementary Fig. 3). The photobleaching of mTq was so pronounced – as seen from an overall signal decrease by approximately 65 % after the first ten repeated scans at 880 nm (see Supplementary Fig. 3) – that it makes it an unlikely choice for fluorescent tagging in single-molecule studies. This observation also invites caution when using mTq in any FRET studies where one expects the molecules to be immobile during their excitation (vs. molecules freely diffusing in solution), as photobleaching more significantly affects molecules that spend longer time within the excitation volume. Nevertheless, in-cell studies of fluorescence recovery after photobleaching could benefit from the propensity of mTq to photobleach.

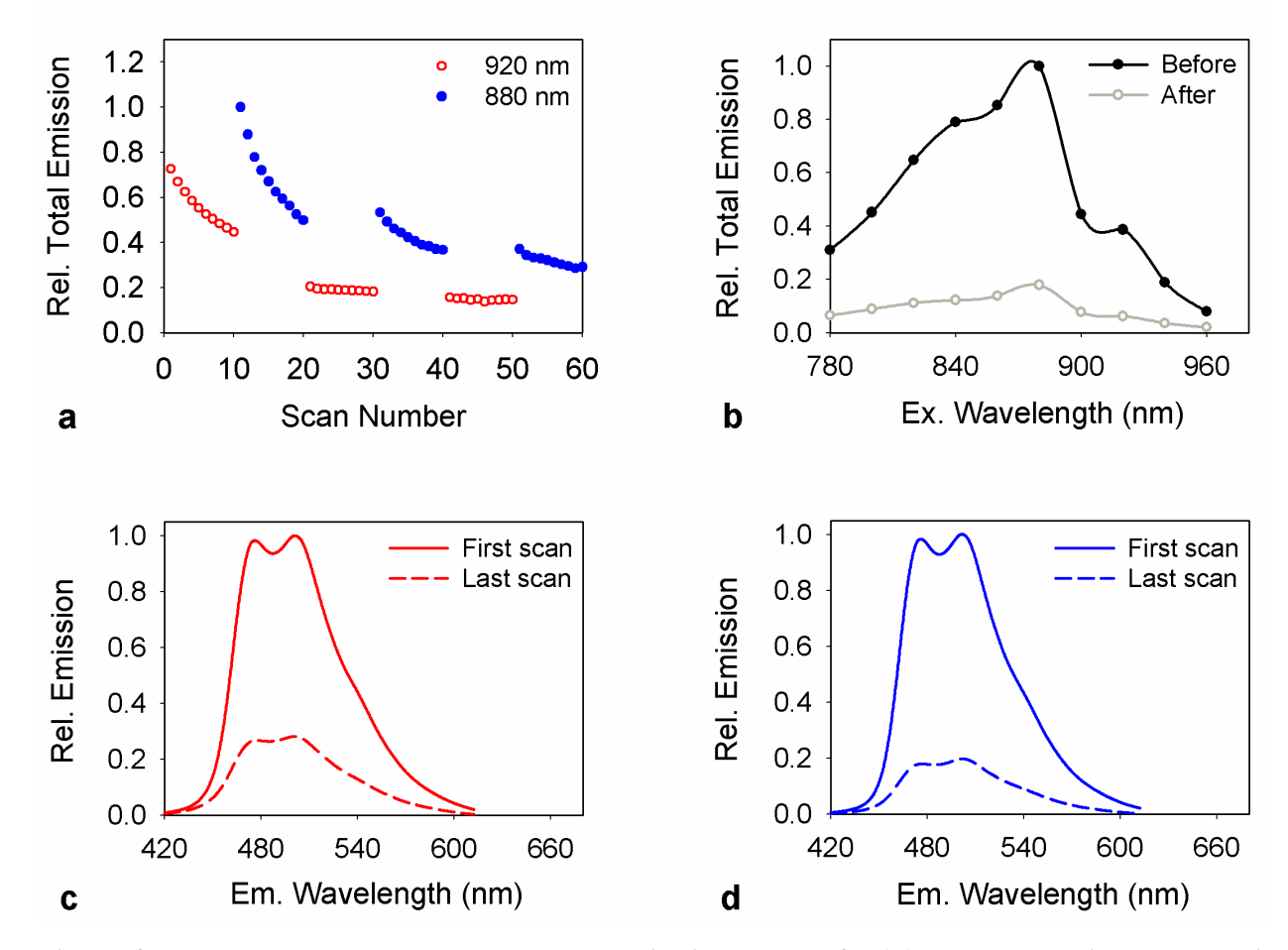


Figure 3. Response to repeated two-photon excitation scans of PAA gel doped with monomeric Turquoise (mTq) fluorescent proteins at pH 8. (a) Changes in total emission intensity induced by acquiring time series of ten successive excitations at 920 nm (empty red circles), followed by ten successive scans at 880 nm (filled blue circles). The couple of 920-nm/880-nm scans was repeated two additional times, for a total of thirty excitation scans at each wavelength. The total emission was computed by integrating over the entire emission spectrum. (b) Comparison of two-photon excitation spectra, measured as emission intensity, before (black line with filled circles) and after (gray line with empty circles) the sample was subjected to the entire excitation time series as shown in (a). (c) Emission spectra of mTq observed at an excitation wavelength of 920 nm, where the red solid line represents the first and the red dashed line represents the last emission spectrum obtained from the repeated excitation time series. (d) Emission spectra of mTq observed upon excitation at 880 nm, where the blue solid line represents the first and the blue dashed line represents the last emission spectrum obtained from the repeated excitation time series. All plots in the figure were normalized relatively to the maximum value observed in the respective data set. The final concentration of mTq in the FP-doped polyacrylamide gel was 1 µM. For repeated excitation time series, the integration time of the camera was 200 ms and the excitation power per entire excitation line was 200 mW (corresponding to 0.5 mW per pixel). For the excitation spectra measurements, the integration time was 50 ms, and the excitation power was 100 mW/line.

Due to the significant amount of photobleaching observed for mTq, we investigated other FPs from the cyan family in order to gauge whether this is a property seen across this entire

subfamily of wtGFP variants. Excitation time series performed on the fluorescent protein mCerulean3, using the pair of excitation wavelengths 920 nm and 886 nm (see Supplementary Fig. 4), reveal once again that a significant amount of photobleaching occurs after repeated scans; specifically, the total fluorescence intensity of mCerulean3 is reduced by more than 61 % after ten repeated scans at 886 nm (see Table 1). In addition, mCerulean3, like mTq, did not show any propensity to photo-switch under 2p excitation at either excitation wavelength. The photobleaching propensity of both mCerulean3 and mTq is potentially a result of the manner in which these FPs (and all of the cyan derivatives of wtGFP for that matter) have been engineered, i.e., by altering the covalent structure of the chromophore through the substitution of amino acids for Tyrosine at amino acid position 66.

In contrast to the wtGFP-derived cyan FPs, which have been engineered via the Y66W substitution in the wtGFP chromophore, there are a number of naturally occurring cyan FPs found in various coral species which possess an anionic tyrosine-derived chromophore that is chemically identical to that of enhanced wtGFP [70]. The challenge posed by many of these naturally occurring cyan FPs found in coral species is that they have a propensity to form strong dimers or even tetramers. Fortunately, optimization of a tetrameric cyan FP found in Clavularia coral (i.e., sp. CFP484 [3]) has led to a monomeric form of the FP, namely monomeric teal fluorescent protein (mTFP1), which is potentially a favorable alternative to wtGFP-derived CFPs with tryptophanderived chromophores such as enhanced CFP or Cerulean [3, 70].

Under two-photon excitation, mTFP1 presents slightly different photophysical properties when compared to mCerulean3 and mTq. The results obtained from performing an excitation time series (using the pair of excitation wavelengths 930 nm and 880 nm) on mTFP1-doped PAA gel are shown in Fig. 4. As seen, mTFP1 is still appreciably photobleached after repeated scans; however, the extent of the photobleaching is noticeably less (total fluorescence intensity was reduced by 47%) compared to the reduction in fluorescence intensity of mTq (65%) and mCerulean3 (61%). Furthermore, mTFP1 was found to be significantly brighter than mTq and mCerulean3, with the relative 2p brightness (relative to mEGFP; see Table 1) of mTFP1 (1.56) nearly two times higher than mTq (0.85) and ~2.5 times higher than mCerulean3. Therefore, it appears that mTFP1 is a favorable alternative to some of the *Aequorea victoria* FPs in the cyan family.

Interestingly, a minute but noticeable, reversible photo-switching effect is also observed for mTFP1. A slight increase in fluorescence signal obtained from 930 nm excitation scans was observed after each set of 890 nm excitation scans was performed (see Fig. 4a). The effect of photo-switching on mGFP2, presented above, manifested itself as a change in the mGFP2 excitation spectrum (Fig. 1b) with no noticeable change in the emission spectrum. However, in the case of mTFP1, the reverse occurred. While no discernible change to the excitation spectrum was detected for mTFP1 (Fig. 4b), the emission spectrum of mTFP1 was altered as a result of repeated excitation scans at 890 nm, in that it became both narrower and red-shifted (see Supplementary Fig. 5). Similar results were obtained after switching the order of the excitation wavelengths in the excitation time series (Supplementary Fig. 6). A more detailed biochemical study of the crystal structures of mTFP1 is needed in order to determine the exact mechanism which causes this slightly altered photophysical behavior when compared with the cyan variants of wtGFP.

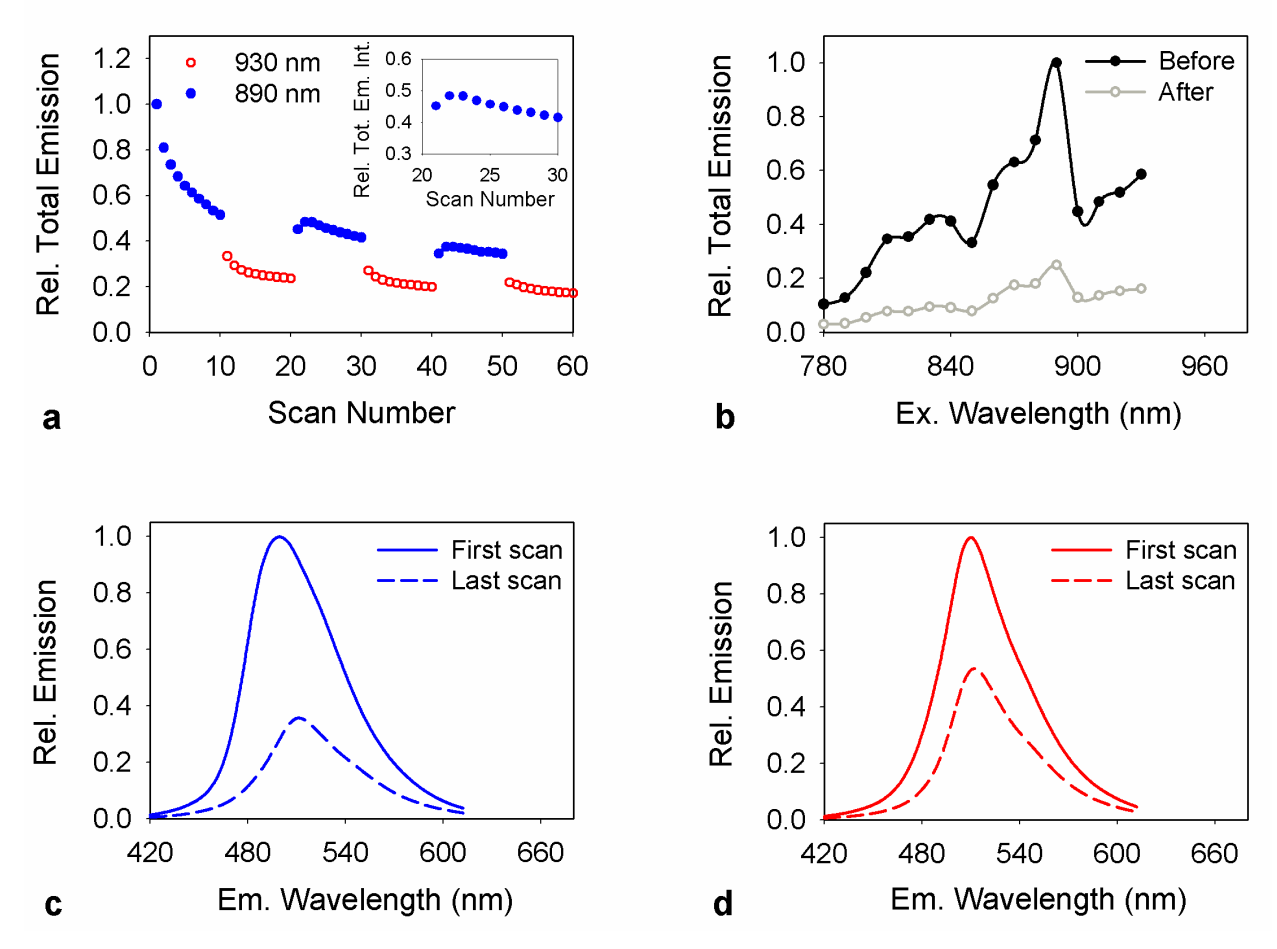


Figure 4. Response to repeated two-photon excitation scans of PAA gel doped with monomeric TFP1 Fluorescent Protein at pH 8. (a) Changes in total emission intensity induced by acquiring time series of ten successive excitation scans at 890 nm (filled blue circles), followed by ten successive excitation scans at 930 nm (empty red circles). The couple of 890-nm/930-nm scans was repeated two additional times, for a total of thirty excitation scans at each wavelength. The total emission was computed by integrating over the entire emission spectrum. The inset displays only the results obtained between scans 10 and scan 40 and serves the purpose of highlighting the increase in emission signal at 930 nm scan due to excitation time series at 890 nm, which most likely occurs due to photo-switching. (b) Comparison of two-photon excitation spectra, measured as emission intensity, before (black line with filled circles) and after (gray line with empty circles) the sample was subjected to the entire excitation time series as shown in (a). (c) Emission spectra observed upon excitation at 890 nm, where the blue solid line represents the first and the blue dashed line represents the last emission spectrum obtained from the repeated time series excitations. (d) Emission spectra observed at an excitation wavelength of 930 nm, where the red solid line represents the first and the red dashed line represents the last emission spectrum obtained from repeated excitation time series. All plots were normalized relatively to the maximum value observed in the respective data set. The final concentration of mTFP1 in the FP-doped polyacrylamide gel was 1 µM. For repeated excitation time series, the integration time of the camera was 200 ms and the excitation power per entire excitation line was 200 mW (corresponding to 0.5 mW per pixel). For the excitation spectra measurements, the integration time was 50 ms and the excitation power was 100 mW/line.

# 3.1.3. Yellow variants of wtGFP

The final subset of wtGFP variants we investigated were those belonging to the yellow fluorescent protein subfamily. The photophysical properties of the monomeric vellow fluorescent protein (mYFP) were probed by exposing mYFP embedded PAA gel to an excitation time series using the pair of excitation wavelengths 960 nm and 800 nm (see Supplementary Fig. 7). A very modest reduction in the fluorescence signal (~9 %) was observed after repeated excitations using the peak excitation wavelength (960 nm) of mYFP. Furthermore, the mYFP excitation spectrum before and after the repeated time series excitation (Supplementary Fig. 7b) were nearly identical, both in overall shape and intensity values. These results indicate that mYFP neither photo-switches nor photobleaches significantly under 2p excitation. These results were identical, i.e., the extent of photobleaching and photo-switching, when switching the order of the excitation wavelengths in the excitation time series (Supplementary Fig. 8). Similar results were obtained for other yellow variants of the wtGFP, i.e., mVenus (Supplementary Fig. 9), mCitrine (Supplementary Fig. 10) and SYFP2 (Supplementary Fig. 11) in that very little photobleaching was observed after subjecting the samples to excitation time series. Within the yellow protein subfamily, the maximum amount of photobleaching (~17%) was observed for SYFP2 after repeated excitation scans at 960 nm; this is still appreciably less than the amount of signal lost due to photobleaching for any of the cyan FPs tested or even for EGFP (see Table 1 for comparisons). Furthermore, there was no photo-switching observed for any of the yellow FPs.

The photo-stable behaviors of the yellow FPs (mYFP, mVenus, mCitrine and SYFP2) we have found using 2p excitation stand in direct contrast to findings of previous studies [51, 71], which have shown that the yellow variants are generally less photostable than mEGFP and the cyan variants when excited using 1p wide-field illumination. Therefore, this photostable behavior of the yellow FPs make them a strong candidate for fluorescent tagging in single-molecule studies as well as in FRET studies which utilize 2p excitation. However, it should be noted, that a major drawback to the palette of FPs in the yellow subfamily of wtGFP variants is that they typically have larger pKa values, especially mYFP (pKa value of 6.9), which make them more susceptible to pH variations in the sample when compared to other subfamilies of wtGFP, and this drawback exists regardless of the choice of excitation.

## 3.2. pH dependence of the photophysical properties of mGFP2

Typical results obtained from performing an excitation time series (using the pair of excitation wavelengths 960 nm and 800 nm) on mGFP2 doped PAA gel at two different pH values (i.e., pH = 6 and pH = 4) are shown in Fig. 5. These results could also be compared to those obtained at pH 8, shown in Fig. 1. As seen, the emission intensity traces for successive excitation scans at 960 nm (open red circles in Fig. 5a-b) were significantly different for different pH values. For pH 6 (see Fig 5a), an increase was observed in total emission intensity under 960-nm excitation (i.e., photoswitching) after successive excitations at 800 nm. The effect of photo-switching at this pH was weaker than that observed at pH 8 (Fig. 1a) and much stronger than seen at pH 4 (see Fig 5b); in the latter case, the effect of photo-switching was completely eliminated, i.e., there was no increase in emission signal under 960-nm excitation following successive excitations at 800 nm. Likewise, the degree of change in the excitation spectrum (see Fig. 1b, 5c-d) decreased with pH. Overall, these changes suggest that mGFP2 chromophore switching from protonated (neutral) to anionic forms occurs less frequently when the pH of the gel was lowered from pH = 8 to pH = 6 and is completely eliminated for pH 4. This result confirms the mechanism underlying the observed

photo-switching: as the pH decreases the concentration of the protonated form of GFP2, relative to the deprotonated form of the molecule will increase, due to the presence of excess H<sup>+</sup> in the gel at low pH. In other words, any photo-switching to the anionic version of the chromophore would be short-lived, due to the composition of the surrounding gel, and therefore the concentration of the protonated form of GFP2 will remain significantly higher than the deprotonated form, even after repeated excitations at 800 nm. Unfortunately, even though there was less photo-switching at low pH, most FPs, including GFP2, lose fluorescence at a pH lower than their neutral pKa, and so it is not practical to use solutions with low pH.

In contrast to the large effect pH had on the ability of mGFP2 to undergo photo-switching, we found no significant change to the extent of photobleaching for mGFP2 samples with pH (cf. Figs. 1 and 5). Specifically, repeated excitations at 800 nm caused a decrease in the total emission intensity for the samples at all three pH values, due, in part, to photobleaching of the sample. For the particular case of the mGFP2 sample, it is difficult to quantify the extent of photobleaching which is occurring as a result of the 800 nm excitations, because the decrease in emission intensity is a result of two factors, photobleaching and photo-switching of some of the chromophores to the anionic state and is difficult to decouple the effects of these two factors. Therefore, it might be the case that there is some small quantitative difference between the exact percentage of molecules which are photobleached in the three different pH cases, although, qualitatively, such differences appear to be minimal.

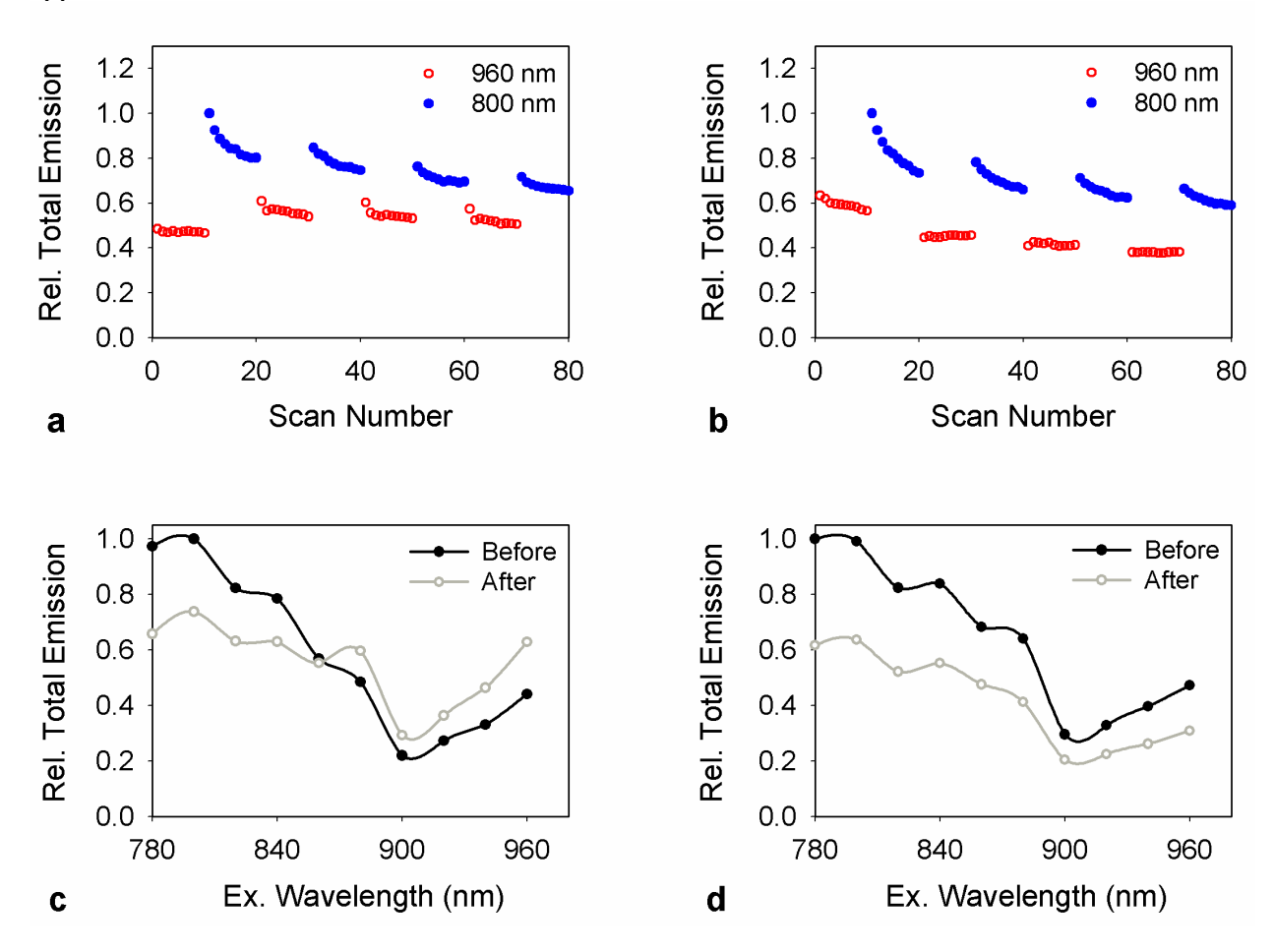


**Figure 5. Effects of pH on photophysical properties of mGFP2 in response to repeated time series excitations. (a-b)** Change in total emission intensity mGFP2 induced by acquiring time series of ten successive excitation scans at 960 nm (empty red circles), followed by ten successive excitation scans at 800 nm (filled blue circles) for mGFP2 doped PAA gel samples at pH values of 6 (panel a) and 4 (panel b), respectively. The couple of 960-nm/800-nm scans was repeated three additional times, for a total of forty excitation scans at each wavelength. **(c-d)** Comparison of excitation spectra before (black line with filled circles) and after (gray line with empty circles) the entire excitation time series as in (a-b) for the sample at pH 6 (panel c) and pH 4 (panel d), respectively. All plots were normalized relatively to the maximum value observed in the respective data set. The final concentration of mGFP2 in the FP-doped polyacrylamide gel was 1 μM. For repeated time series excitations, the integration time of the camera was 200 ms and the excitation power per entire excitation line was 200 mW (corresponding to 0.5 mW per pixel). For the excitation spectra measurements, the integration time was 50 ms and the excitation power was 100 mW/line.

## 3.3. Relative brightness of FPs under two-photon excitation

In addition to photostability, the intrinsic brightness, which is linearly proportional to the number of photons an FP emits per measurement period, is a vital characteristic to keep in mind when selecting the correct FP to use. The intrinsic brightness of any fluorescent molecule depends on two properties of the molecule, namely the extinction coefficient (or the excitation cross-section) of the FP, which is a measure of the ability of the FP to absorb light, and the quantum yield, which is a measure of the efficiency of photon emission once the FP is in an excited state. These properties could be affected by various environmental as well as instrumental factors such as pH, temperature, excitation light intensity, and wavelength.

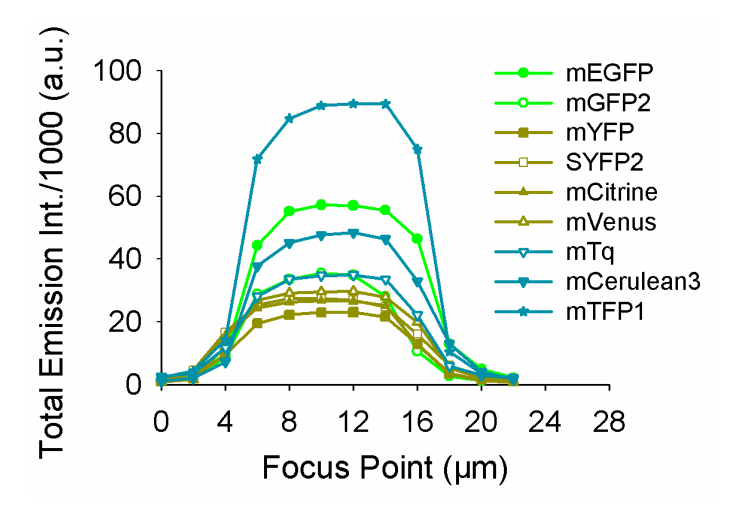


Figure 6. Comparison of the total emission intensity of a variety of FPs. The FP-doped polyacrylamide gel samples were prepared using DPBS buffer (pH = 8) with a final FP concentration of 1  $\mu$ M. Z-stack acquisitions (see Methods section) were taken for each FP sample with an average power of 12 mW/point and at integration time of 100 ms. The excitation wavelength chosen for the z-stack acquisitions corresponded to the peak of the respective FP's excitation spectra, as described above.

Because the brightness of an FP depends on an array of different parameters, in this work, we sought to determine the relative 2p brightness of all the FPs which have been investigated in this study by using the same acquisition settings and sample preparation protocol for each. In order

to accomplish this, each prepared sample of PAA gel-embedded FP was scanned by focused light at different depths and the fluorescence intensity determined at each depth, to create a "sample uniformity curve" (see Fig. 6). The purpose of the uniformity curve was to assure that the FPs were not distributed inhomogeneously throughout the sample, which would negate one of the crucial parameters which needs to remain constant for a proper comparison of brightness values, i.e., the concentration of the sample. Only emission intensity profiles were used for further analysis that formed a plateau which consisted of at least four approximately equal total emission intensity values acquired from consecutive planes in the center of the gel sample. The decrease in intensity on both sides of the plateau was due to the decrease in the overlap between the point spread function of the focused light and the sample film.

We have defined the 2p relative brightness to be the ratio of total emission intensity of an FP to that of mEGFP, whereas total emission intensity was found by averaging the results of the multiple measurements along the plateau of the uniformity curve. Based on the total emission intensities, the fluorescent protein mTFP1 is the brightest of the measured FPs followed by mEGFP, mCerulean3, mTq, mGFP2, mVenus, SYFP2, mCitrine, and mYFP (see Fig. 6). The results of this assay are summarized in Table 1, alongside with those regarding photobleaching and photo-switching described in previous sections. Interestingly, the results shown in Table 1 reveal that the relative brightness of the various FP subfamilies using 2p excitation are significantly different than the relative brightness values of the FPs determined using 1p excitation. For example, the yellow subfamily of proteins is the brightest using 1p excitation, but the dimmest using 2p excitation.

**Table 1. Summary of photophysical properties of FPs investigated in this study**. Values resulting from 2p excitation were determined as described in this work, while those resulting from 1p excitation, as well as pKa values and lists of mutations were obtained from the literature (indicated in the column for 1p Brightness).

		1		,			
FP	pKa	$\epsilon^*$	Q*	1p Relative	2p Relative	2p Photo-	2p Photo-
		$(m^{-1}M^{-1})$		Brightness*	Brightness <sup>†</sup>	bleaching <sup>‡</sup>	switching
mEGFP <sup>a</sup>	6.0	56,000	0.60	1.00 [3, 5]	$1.00 \pm 0.06$	$0.25\pm0.09$	No
mGFP2 <sup>b</sup>	-	21,000	0.55	0.34 [6, 8]	$0.63 \pm 0.06$	-	Yes
mYFP <sup>c</sup>	6.9	83,400	0.61	1.51 [5, 65]	$0.41 \pm 0.05$	$0.09 \pm 0.07$	No
mVenus <sup>d</sup>	6.0	92,200	0.57	1.56 [52, 54]	$0.52\pm0.04$	$0.11 \pm 0.05$	No
SYFP2 <sup>e</sup>	6.0	101,000	0.68	2.04 [54]	$0.50 \pm 0.04$	$0.17 \pm 0.09$	No
mCitrine <sup>f</sup>	5.7	77,000	0.76	1.74 [52, 53]	$0.47 \pm 0.12$	$0.03 \pm 0.02$	No
mCerulean3g	3.3	40,000	0.87	1.03 [7]	$0.85 \pm 0.09$	$0.61 \pm 0.06$	No
mTq <sup>h</sup>	4.5	30,000	0.84	0.75 [55]	$0.63 \pm 0.03$	$0.65 \pm 0.04$	No
mTFP1 <sup>#</sup>	4.3	64,000	0.85	1.60 [3]	$1.56 \pm 0.07$	$0.47 \pm 0.02$	Yes

Notes: \*Relative to the brightness of mEGFP, which is 33,600 m<sup>-1</sup>M<sup>-1</sup>for 1p excitation. 1p brightness was calculated by multiplying the extinction coefficient (ε) and quantum yield (Q). †Observed emission intensity for given FP at pH 8 relative to the observed emission intensity of mEGFP. ‡Fraction of total fluorescence bleached from first 10 excitation scans using the specific peak excitation wavelength of each FP. The variants of green fluorescent protein incorporated the following mutations relative to the wild-type: a mEGFP: F64L, S65T, A206K; b mGFP2: F64L, A206K; c mYFP: S65G, V68L, Q69K, S72A, T203Y,

A206K; <sup>d</sup>mVenus: F46L, F64L, S65G, V68L, S72A, M153T, V163A, S175G, T203Y, A206K; <sup>e</sup> SYFP2: F46L, F64L, S65G, S72A, M153T, V163A, S175G, T203Y, A206K; <sup>f</sup> mCitrine: S65G, V68L, Q69M, S72A, T203Y, A206K; <sup>g</sup> mCerulean3: F64L, Y66W, S72A, Y145A, N146T, S147H, H148G, M153T, V163A, K166G, I167L, R168N, H169C, A206K; <sup>h</sup>mTq: F64L, Y66W, S72A, N146I, H148D, M153T, V163A, S175F, A206K. <sup>#</sup>mTFP1: a variant of cFP484

#### 4. CONCLUSION

Having knowledge of photophysical properties of fluorescent proteins (FPs), such as emission and absorption spectra, brightness, photostability, and photo-switching properties, is very helpful in choosing compatible FPs for a particular application. In past two decades, studies have led to a plethora of new FPs with improved photophysical properties and have spurred the development of robust fluorescence-based tools and techniques designed for 2p excitation and numerous applications of those techniques. However, information on the photophysical properties of many FPs under 2p excitation has remained somewhat limited.

Along with the experimental parameters used in the imaging system (power, wavelength, spectral resolution, and exposure time), the source of illumination and detector used in an imaging system could also alter the observed intensity of the fluorescent molecules. Our comparative analysis of the photophysical properties of a large number of widely used FPs provided some interesting insights.

Of the FPs studied in this work, we found that mEGFP is the brightest among those which have been derived from wtGFP, and it exhibited only moderate photobleaching and no noticeable photo-switching under 2p excitation. Because of these features, mEGFP is one of the best options for those fluorescence applications that require high photostability and brightness such as FRET [9, 21, 38] and Number and Brightness (N&B) analysis [72]. Nevertheless, other factors may factor in when choosing a good FRET pair for a certain experiment, including good separation between donor and acceptor emission spectra, which is necessary in imaging experiments without spectral resolution. Another green variant of wtGFP, GFP2, exhibited strong irreversible photo-switching from one sub-population (excitation state) to another, which are excited maximally by different wavelengths. This photo-switching effect significantly depends on the pH of the sample.

Cyan variants of wtGFP, namely mCerulean3 and mTq showed high propensities to photobleach with no significant effect of photo-switching. This observed result suggests that mTq and Cerulean3 could be appropriate options for the FRAP experiments because of their high propensity to photobleach. These FPs (i.e., mTq, and mCerulean3) were brighter than all the yellow variants of wtGFP measured in this study. Another Cyan FP (but derived from CFP484 [3]), mTFP1, is the brightest among the measured FPs in this investigation. Based on our measurements, mTFP1 exhibits a pronounced effect of photobleaching; however, not as pronounced as the other cyan FPs. In addition to that, a minute but noticeable, irreversible photoswitching from one fluorescence color to another was observed under 2p excitation on PAA geldoped mTFP1.

The yellow variants of the wtGFP measured in this investigation, namely mCitrine, mYFP, mVenus, and SYFP2 were dimmer than both green variants and cyan variants tested in this study. Among these yellow variants of wtGFP, we found mVenus is brightest and mYFP is the dimmest under 2p excitation. This entire subclass of FPs showed a small effect of photobleaching with essentially no effect of photo-switching under 2p excitations. Based on these results we conclude

that yellow FPs studied here are likely to be a good choice for measurements that require strong photostability.

Based on those observations, we note that the choice of FPs depends on the specific application considered. For instance, for FRAP studies one could choose cyan variants, while for applications that require switching, GFP2 and perhaps mTFP1 could be used. At the same time, for experiments where steady, long-lasting fluorescence is needed, there are several choices available. Even in this case, FPs that exhibit photo-switching and photobleaching may still be used by choosing less intense laser light with an excitation wavelength that minimizes photobleaching and photo-switching while maintaining a relatively high brightness, if applications do not require FP immobilization under continuous excitation.

In conclusion, our study adds to the body of evidence that the specific photophysical properties of fluorescent proteins under two-photon excitation, including excitation and emission spectra as well as their propensity to undergo light-induced changes, may not be simply inferred from one photon excitation. Lack of knowledge or appreciation of such properties may lead to erroneous conclusions in, e.g., FRET studies [69]. Thus, the choice of fluorescent proteins for a particular experiment depends, among other things, on whether one uses single- or two-photon excitation. We propose that, whenever possible, FP developers incorporate 2p properties in the spec sheets of their FPs in the future.

**ACKNOWLEDGEMENTS** We thank Prof. Brent Hoffman (Duke University) for kindly providing the mTFP1 plasmid. This work was partly supported by grants from the National Science Foundation (grant numbers PHY-1626450 and DBI-1919670) as well as from the UWM Research Growth Initative (101X396) awarded to V.R. and I.P., and from NSF Career Award (MCB-1846143) awarded to I.P.

## 5. REFERENCES

- [1] O. Shimomura, F.H. Johnson, Y. Saiga, Extraction, purification and properties of aequorin, a bioluminescent protein from the luminous hydromedusan, Aequorea, Journal of cellular and comparative physiology, 59(3) (1962) 223-239.
- [2] M.V. Matz, A.F. Fradkov, Y.A. Labas, A.P. Savitsky, A.G. Zaraisky, M.L. Markelov, S.A. Lukyanov, Fluorescent proteins from nonbioluminescent Anthozoa species, Nat Biotechnol, 17 (1999) 969-973.
- [3] H.W. Ai, J.N. Henderson, S.J. Remington, R.E. Campbell, Directed evolution of a monomeric, bright and photostable version of Clavularia cyan fluorescent protein: structural characterization and applications in fluorescence imaging, Biochem J, 400 (2006) 531-540.
- [4] R. Heim, A.B. Cubitt, R.Y. Tsien, Improved Green Fluorescence, Nature, 373 (1995) 663-664.
- [5] A.B. Cubitt, R. Heim, S.R. Adams, A.E. Boyd, L.A. Gross, R.Y. Tsien, Understanding, Improving and Using Green Fluorescent Proteins, Trends Biochem Sci, 20 (1995) 448-455.
- [6] T. Zimmermann, J. Rietdorf, A. Girod, V. Georget, R. Pepperkok, Spectral imaging and linear unmixing enables improved FRET efficiency with a novel GFP2-YFP FRET pair, Febs Lett, 531 (2002) 245-249.
- [7] M.L. Markwardt, G.J. Kremers, C.A. Kraft, K. Ray, P.J.C. Cranfill, K.A. Wilson, R.N. Day, R.M. Wachter, M.W. Davidson, M.A. Rizzo, An Improved Cerulean Fluorescent Protein with Enhanced Brightness and Reduced Reversible Photoswitching, Plos One, 6 (2011) e17896.
- [8] V. Raicu, M.R. Stoneman, R. Fung, M. Melnichuk, D.B. Jansma, L.F. Pisterzi, S. Rath, M. Fox, J.W. Wells, D.K. Saldin, Determination of supramolecular structure and spatial distribution of protein complexes in living cells, Nat Photonics, 3 (2009) 107-113.

- [9] M. Parsons, B. Vojnovic, S. Ameer-Beg, Imaging protein-protein interactions in cell motility using fluorescence resonance energy transfer (FRET), Biochem Soc T, 32 (2004) 431-433.
- [10] J. Widengren, R. Rigler, Review Fluorescence correlation spectroscopy as a tool to investigate chemical reactions in solutions and on cell surfaces, Cell Mol Biol, 44 (1998) 857-879.
- [11] Stoneman MR, Biener G, Ward RJ, Pediani JD, Badu D, Eis A, Popa I, Milliagn G, Raicu V., A general method to quantify lignad-driven oligomerization from fluorescence-based images, Nat Methods, 16 (2019) 493-496.
- [12] M.R. Stoneman, G. Biener, V. Raicu, Reply to: Spatial heterogeneity in molecular brightness, Nat Methods, 17 (2020) 276-278.
- [13] V. Raicu, D.B. Jansma, R.J.D. Miller, J.D. Friesen, Protein interaction quantified in vivo by spectrally resolved fluorescence resonance energy transfer, Biochem J, 385 (2005) 265-277.
- [14] V. Zinchuk, O. Zinchuk, T. Okada, Quantitative colocalization analysis of multicolor confocal immunofluorescence microscopy images: Pushing pixels to explore biological phenomena, Acta Histochem Cytoc, 40 (2007) 101-111.
- [15] N. Ariotti, T.E. Hall, J. Rae, C. Ferguson, K.A. McMahon, N. Martel, R.E. Webb, R.I. Webb, R.D. Teasdale, R.G. Parton, Modular Detection of GFP-Labeled Proteins for Rapid Screening by Electron Microscopy in Cells and Organisms, Dev Cell, 35 (2015) 513-525.
- [16] M. Mastop, D.S. Bindels, N.C. Shaner, M. Postma, T.W.J. Gadella, J. Goedhart, Characterization of a spectrally diverse set of fluorescent proteins as FRET acceptors for mTurquoise2, Sci Rep-Uk, 7 (2017).
- [17] J. Paprocki, G. Biener, M. Stoneman, V. Raicu, In-Cell Detection of Conformational Substates of a G Protein-Coupled Receptor Quaternary Structure: Modulation of Substate Probability by Cognate Ligand Binding, J Phys Chem B, 124 (2020) 10062-10076.
- [18] D.R. Singh, P. Kanvinde, C. King, E.B. Pasquale, K. Hristova, The EphA2 receptor is activated through induction of distinct, ligand-dependent oligomeric structures (vol 1, 15, 2018), Commun Biol, 1 (2018).
- [19] C. King, M. Stoneman, V. Raicu, K. Hristova, Fully quantified spectral imaging reveals in vivo membrane protein interactions, Integr Biol-Uk, 8 (2016) 216-229.
- [20] V. Vu, T. Ligh, B. Sullivan, D. Greiner, K. Hristova, D. Leckband, P120 catenin potentiates constitutive E-cadherin dimerization at the plasma membrane and regulates trans binding, Current Biology, (2021).
- [21] E.A. Jares-Erijman, T.M. Jovin, FRET imaging, Nat Biotechnol, 21 (2003) 1387-1395.
- [22] R.V. Shivnaraine, D.D. Fernandes, H.Q. Ji, Y.C. Li, B. Kelly, Z.F. Zhang, Y.R. Han, F. Huang, K.S. Sankar, D.N. Dubins, J.V. Rocheleau, J.W. Wells, C.C. Gradinaru, Single-Molecule Analysis of the Supramolecular Organization of the M-2 Muscarinic Receptor and the G alpha(i1) Protein, J Am Chem Soc, 138 (2016) 11583-11598.
- [23] Y. Chen, N.C. Deffenbaugh, C.T. Anderson, W.O. Hancock, Molecular counting by photobleaching in protein complexes with many subunits: best practices and application to the cellulose synthesis complex, Mol Biol Cell, 25 (2014) 3630-3642.
- [24] M. Drobizhev, N.S. Makarov, S.E. Tillo, T.E. Hughes, A. Rebane, Two-photon absorption properties of fluorescent proteins, Nat Methods, 8 (2011) 393-399.
- [25] A.J. Lam, F. St-Pierre, Y.Y. Gong, J.D. Marshall, P.J. Cranfill, M.A. Baird, M.R. McKeown, J. Wiedenmann, M.W. Davidson, M.J. Schnitzer, R.Y. Tsien, M.Z. Lin, Improving FRET dynamic range with bright green and red fluorescent proteins, Nat Methods, 9 (2012) 1005-+.
- [26] Z.F. Wang, J.V. Shah, Z.P. Chen, C.H. Sun, M.W. Berns, Fluorescence correlation spectroscopy investigation of a GFP mutant-enhanced cyan fluorescent protein and its tubulin fusion in living cells with two-photon excitation, J Biomed Opt, 9 (2004) 395-403.
- [27] M. Cotlet, P.M. Goodwin, G.S. Waldo, J.H. Werner, A comparison of the fluorescence dynamics of single molecules of a green fluorescent protein: One- versus two-photon excitation, Chemphyschem, 7 (2006) 250-260.

- [28] H.E. Grecco, K.A. Lidke, R. Heintzmann, D.S. Lidke, C. Spagnuolo, O.E. Martinez, E.A. Jares-Erijman, T.M. Jovin, Ensemble and single particle photophysical proper-ties (Two-Photon excitation, anisotropy, FRET, lifetime, spectral conversion) of commercial quantum dots in solution and in live cells, Microsc Res Techniq, 65 (2004) 169-179.
- [29] M. Drobizhev, S. Tillo, N.S. Makarov, T.E. Hughes, A. Rebane, Absolute Two-Photon Absorption Spectra and Two-Photon Brightness of Orange and Red Fluorescent Proteins, J Phys Chem B, 113 (2009) 855-859.
- [30] B.L. Grigorenko, A.V. Nemukhin, I.V. Polyakov, M.G. Khrenova, A.I. Krylov, A Light-Induced Reaction with Oxygen Leads to Chromophore Decomposition and Irreversible Photobleaching in GFP-Type Proteins, J Phys Chem B, 119 (2015) 5444-5452.
- [31] T. Bernas, J.P. Robinson, E.K. Asem, B. Rajwa, Loss of image quality in photobleaching during microscopic imaging of fluorescent probes bound to chromatin, J Biomed Opt, 10 (2005) 064015.
- [32] D.M. Chudakov, V.V. Verkhusha, D.B. Staroverov, E.A. Souslova, S. Lukyanov, K.A. Lukyanov, Photoswitchable cyan fluorescent protein for protein tracking, Nat Biotechnol, 22 (2004) 1435-1439.
- [33] X.X. Zhou, M.Z. Lin, Photoswitchable fluorescent proteins: ten years of colorful chemistry and exciting applications, Curr Opin Chem Biol, 17 (2013) 682-690.
- [34] J. Lippincott-Schwartz, G.H. Patterson, Photoactivatable fluorescent proteins for diffraction-limited and super-resolution imaging, Trends Cell Biol, 19 (2009) 555-565.
- [35] D. Bourgeois, V. Adam, Reversible photoswitching in fluorescent proteins: A mechanistic view, Iubmb Life, 64 (2012) 482-491.
- [36] K.A. Lukyanov, D.M. Chudakov, S. Lukyanov, V.V. Verkhusha, Photoactivatable fluorescent proteins, Nat Rev Mol Cell Bio, 6 (2005) 885-891.
- [37] J.J. van Thor, A.J. Pierik, I. Nugteren-Roodzant, A.H. Xie, K.J. Hellingwerf, Characterization of the photoconversion of green fluorescent protein with FTIR spectroscopy, Biochemistry-Us, 37 (1998) 16915-16921.
- [38] V. Raicu, D.R. Singh, FRET Spectrometry: A New Tool for the Determination of Protein Quaternary Structure in Living Cells, Biophys J, 105 (2013) 1937-1945.
- [39] F. Ahmed, E. Zapata-Mercado, S. Rahman, K. Hristova, The Biased Ligands NGF and NT-3 Differentially Stabilize Trk-A Dimers, Biophys J, 120 (2021) 55-63.
- [40] O. Krichevsky, G. Bonnet, Fluorescence correlation spectroscopy: the technique and its applications, Rep Prog Phys, 65 (2002) 251-297.
- [41] B.L. Sprague, J.G. McNally, FRAP analysis of binding: proper and fitting, Trends Cell Biol, 15 (2005) 84-91.
- [42] D.M. Chudakov, S. Lukyanov, K.A. Lukyanov, Tracking intracellular protein movements using photoswitchable fluorescent proteins PS-CFP2 and Dendra2, Nat Protoc, 2 (2007) 2024-2032.
- [43] V. Adam, H. Mizuno, A. Grichine, J.I. Hotta, Y. Yamagata, B. Moeyaert, G.U. Nienhaus, A. Miyawaki, D. Bourgeois, J. Hofkens, Data storage based on photochromic and photoconvertible fluorescent proteins, J Biotechnol, 149 (2010) 289-298.
- [44] J.K. Heppert, D.J. Dickinson, A.M. Pani, C.D. Higgins, A. Steward, J. Ahringer, J.R. Kuhn, B. Goldstein, Comparative assessment of fluorescent proteins for in vivo imaging in an animal model system, Mol Biol Cell, 27 (2016) 3385-3394.
- [45] P.J. Cranfill, B.R. Sell, M.A. Baird, J.R. Allen, Z. Lavagnino, H.M. de Gruiter, G.J. Kremers, M.W. Davidson, A. Ustione, D.W. Piston, Quantitative assessment of fluorescent proteins, Nat Methods, 13 (2016) 557-562.
- [46] M.R. Stoneman, N. Raicu, G. Biener, V. Raicu, Fluorescence-based Methods for the Study of Protein-Protein Interactions Modulated by Ligand Binding, Current Pharmaceutical Design, 26 (2020) 5668-5683.
- [47] K. Haubert, T. Drier, D. Beebe, PDMS bonding by means of a portable, low-cost corona system, Lab Chip, 6 (2006) 1548-1549.

- [48] M. Stoneman, M. Fox, C.Y. Zeng, V. Raicu, Real-time monitoring of two-photon photopolymerization for use in fabrication of microfluidic devices, Lab Chip, 9 (2009) 819-827.
- [49] B.P. Cormack, R.H. Valdivia, S. Falkow, FACS-optimized mutants of the green fluorescent protein (GFP), Gene, 173 (1996) 33-38.
- [50] M. Kneen, J. Farinas, Y.X. Li, A.S. Verkman, Green fluorescent protein as a noninvasive intracellular pH indicator, Biophys J, 74 (1998) 1591-1599.
- [51] N.C. Shaner, P.A. Steinbach, R.Y. Tsien, A guide to choosing fluorescent proteins, Nat Methods, 2 (2005) 905-909.
- [52] N.C. Shaner, Fluorescent proteins for quantitative microscopy: Important properties and practical evaluation, Method Cell Biol, 123 (2014) 95-111.
- [53] O. Griesbeck, G.S. Baird, R.E. Campbell, D.A. Zacharias, R.Y. Tsien, Reducing the environmental sensitivity of yellow fluorescent protein Mechanism and applications, J Biol Chem, 276 (2001) 29188-29194.
- [54] G.J. Kremers, J. Goedhart, E.B. van Munster, T.W.J. Gadella, Cyan and yellow super fluorescent proteins with improved brightness, protein folding, and FRET Forster radius, Biochemistry-Us, 45 (2006) 6570-6580.
- [55] J. Goedhart, L. van Weeren, M.A. Hink, N.O.E. Vischer, K. Jalink, T.W.J. Gadella, Bright cyan fluorescent protein variants identified by fluorescence lifetime screening, Nat Methods, 7 (2010) 137-U174.
- [56] D.A. Zacharias, J.D. Violin, A.C. Newton, R.Y. Tsien, Partitioning of lipid-modified monomeric GFPs into membrane microdomains of live cells, Science, 296 (2002) 913-916.
- [57] R.M. Dickson, D.J. Norris, Y.L. Tzeng, W.E. Moerner, Three-dimensional imaging of single molecules solvated in pores of poly(acrylamide) gels, Science, 274 (1996) 966-969.
- [58] K. Weber, M. Osborn, SDS-PAGE to determine the molecular weight of proteins: The work of Klaus Weber and Mary Osborn The reliability of molecular weight determinations by dodecyl sulfate-polyacrylamide gel electrophoresis (reprinted from J.Biol. Chem. vol. 244, pg. 4406-4412, 1969), J Biol Chem, 281 (2006).
- [59] G. Biener, M.R. Stoneman, G. Acbas, J.D. Holz, M. Orlova, L. Komarova, S. Kuchin, V. Raicu, Development and Experimental Testing of an Optical Micro-Spectroscopic Technique Incorporating True Line-Scan Excitation, Int J Mol Sci, 15 (2014) 261-276.
- [60] A.K. Mishra, M. Gragg, M.R. Stoneman, G. Biener, J.A. Oliver, P. Miszta, S. Filipek, V. Raicu, P.S.H. Park, Quaternary structures of opsin in live cells revealed by FRET spectrometry, Biochem J, 473 (2016) 3819-3836.
- [61] M.R. Stoneman, J.D. Paprocki, G. Biener, K. Yokoi, A. Shevade, S. Kuchin, V. Raicu, Quaternary structure of the yeast pheromone receptor Ste2 in living cells, Bba-Biomembranes, 1859 (2017) 1456-1464.
- [62] S. Marsango, G. Caltabiano, M. Jimemez-Roses, M.J. Millan, J.D. Pediani, R.J. Ward, G. Milligan, A Molecular Basis for Selective Antagonist Destabilization of Dopamine D-3 Receptor Quaternary Organization, Sci Rep-Uk, 7 (2017) 1-17.
- [63] R.J. Ward, J.D. Pediani, S. Marsango, R. Jolly, M.R. Stoneman, G. Biener, T.M. Handel, V. Raicu, G. Milligan, Chemokine receptor CXCR4 oligomerization is disrupted selectively by the antagonist ligand IT1t, Journal of Biological Chemistry, 296 (2021) 100139.
- [64] S. Patowary, L.F. Pisterzi, G. Biener, J.D. Holz, J.A. Oliver, J.W. Wells, V. Raicu, Experimental Verification of the Kinetic Theory of FRET Using Optical Microspectroscopy and Obligate Oligomers, Biophys J, 108 (2015) 1613-1622.
- [65] T.B. McAnaney, W. Zeng, C.F.E. Doe, N. Bhanji, S. Wakelin, D.S. Pearson, P. Abbyad, X.H. Shi, S.G. Boxer, C.R. Bagshaw, Protonation, photobleaching, and photoactivation of yellow fluorescent protein (YFP 10C): A unifying mechanism, Biochemistry-Us, 44 (2005) 5510-5524.
- [66] G.H. Patterson, J. Lippincott-Schwartz, A photoactivatable GFP for selective photolabeling of proteins and cells, Science, 297 (2002) 1873-1877.

- [67] K. Brejc, T.K. Sixma, P.A. Kitts, S.R. Kain, R.Y. Tsien, M. Ormo, S.J. Remington, Structural basis for dual excitation and photoisomerization of the Aequorea victoria green fluorescent protein, P Natl Acad Sci USA, 94 (1997) 2306-2311.
- [68] R. Heim, D.C. Prasher, R.Y. Tsien, Wavelength Mutations and Posttranslational Autoxidation of Green Fluorescent Protein, P Natl Acad Sci USA, 91 (1994) 12501-12504.
- [69] V. Raicu, Ab inito derivation of the FRET equations resolves old puzzles and suggests measurement strategies, Biophys J, 116, 1313-1327 (2019).
- [70] H.W. Ai, S.G. Olenych, P. Wong, M.W. Davidson, R.E. Campbell, Hue-shifted monomeric variants of Clavularia cyan fluorescent protein: identification of the molecular determinants of color and applications in fluorescence imaging, Bmc Biol, 6 (2008).
- [71] R.N. Day, M.W. Davidson, The fluorescent protein palette: tools for cellular imaging, Chem Soc Rev, 38 (2009) 2887-2921.
- [72] N.G. James, M.A. Digman, E. Gratton, B. Barylko, X.D. Ding, J.P. Albanesi, M.S. Goldberg, D.M. Jameson, Number and Brightness Analysis of LRRK2 Oligomerization in Live Cells, Biophys J, 102 (2012) A41-A43.